Electronic Supplementary Information (ESI)

AIE-active Iridium(III) Complex Integrated with Upconversion Nanoparticles for NIR-irradiated Photodynamic Therapy

Shengnan Liu,[‡a] Jiahong Han,[‡a] Yulei Chang,[*b] Weijin Wang,[a] Runlin Wang,[a] Ziwei Wang,[a] Guangzhe Li,[*c] Dongxia Zhu[*a] and Martin R. Bryce[*d]

[a] *Key Laboratory of Nanobiosensing and Nanobioanalysis at Universities of Jilin Province, Department of Chemistry, Northeast Normal University, 5268 Renmin Street, Changchun, Jilin Province 130024, P. R. China.*

E-mail: zhudx047@nenu.edu.cn

[b] *State Key Laboratory of Luminescence and Applications, Changchun Institute of Optics, Fine Mechanics and Physics, Chinese Academy of Sciences, Changchun Jilin Province 130033, China.*

Email: yuleichang@ciomp.ac.cn

[c] *Jilin Provincial Science and Technology Innovation Center of Health Food of Chinese Medicine, Changchun University of Chinese Medicine, Changchun, Jilin Province 130117, P. R. China.*

E-mail: 1993008106@qq.com

[d] *Department of Chemistry, Durham University, Durham, DH1 3LE, UK.*

E-mail: m.r.bryce@durham.ac.uk

‡*The authors contributed equally to the preparation of this work.*

Table of Contents

Experimental Section

Materials and instruments

Materials for organic synthesis, poloxamer (F127) and indocyanine green (ICG) were purchased from Energy Chemical Company. RPMI Medium 1640 was purchased from Solarbio Life Science company. Fetal bovine serum (FBS) was purchased from Sigma-Aldrich. 3-(4,5-Dimethylthiazol-2-yl)-2,5-diphenyltetrazolium bromide (MTT) was obtained from Aladdin. 2',7'-Dichlorofluorescence diacetate (DCFH-DA) and the cell viability (live dead cell staining) assay kit were purchased from Shanghai Beyotime Biotechnology Co.,Ltd.

^{1}H NMR spectra was recorded at 25 °C on a Varian 500 MHz spectrometer. The high resolution mass spectrometry (HRMS) was obtained on a high-performance liquid chromatography-high-resolution time of flight mass spectrometer (MicrOTOF II). UV-vis absorption spectra were recorded on a Shimadzu UV-3100 spectrophotometer. The photoluminescence spectra, excited state lifetimes (τ) and photoluminescence quantum yields (Φ_{PL}) were recorded on an Edinburgh FLS920 spectrofluorimeter under air at room temperature. Transmission electron microscopy (TEM) images of the samples were taken by a TECNAI F20 microscope. Diameter and diameter distribution of the nanoparticles were determined by a Malvern Zetasizer Nano instrument for dynamic light scattering (DLS). Confocal laser scanning microscopy (CLSM) images were taken using a ZeissLSM 700 (Zurich, Switzerland).

Synthesis of L1

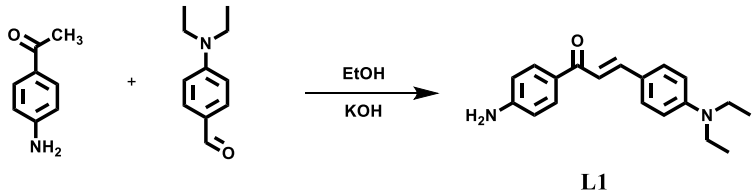

L1

Scheme S1. Synthetic route for **L1**.

According to the literature,[1] 4-aminoacetophenone (0.540 g, 4 mmol) and *N,*

N-diethyl-4-aminobenzaldehyde (0.708 g, 4 mmol) were dissolved in ethanol (40 mL) and 10% KOH solution (20 mL) was added. The reaction was stirred at RT for 24 h. After completion of the reaction, extraction was performed with CH_2Cl_2 to remove KOH, and the organic layer was dried over anhydrous Na_2SO_4. The solvent was removed by a rotary evaporator. Using ethyl acetate and petroleum ether as eluents (ethyl acetate/petroleum ether from 1/10 to 1/1, v/v), the crude product was purified by silica gel column chromatography to obtain a yellow solid product. Yield: 43%. ^{1}H NMR (500 MHz, $CDCl_3$, δ [ppm]): 7.95-7.89 (m, 2H), 7.76 (d, *J* = 15.4 Hz, 1H), 7.52 (d, *J* = 8.8 Hz, 2H), 7.33 (d, *J* = 15.4 Hz, 1H), 6.72-6.63 (m, 4H), 4.10 (s, 2H), 3.41 (q, *J* = 7.1 Hz, 4H), 1.20 (t, *J* = 7.1 Hz, 6H).

Synthesis of L2

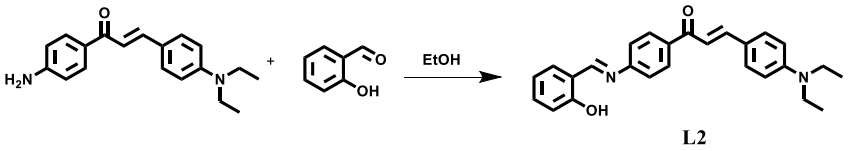

L2

Scheme S2. Synthetic route for **L2**.

The auxiliary ligand **L2** was synthesized by a simple and high-yielding Schiff base reaction. Aminochalcone (0.088 g, 0.3 mmol) and *o*-hydroxybenzaldehyde (0.108 g, 0.9 mmol) were added into ethanol (30 mL). The mixture were heated to 78 °C and refluxed with stirring for 8 h to give an orange precipitate. The reaction mixture was cooled to room temperature. The precipitate was filtered to obtain auxiliary ligand **L2**. Yield: 90%. ^{1}H NMR (500 MHz, $CDCl_3$, δ [ppm]): 13.03 (s, 1H), 8.67 (s, 1H), 8.13-8.07 (m, 2H), 7.82 (d, *J* = 15.3 Hz, 1H), 7.55 (d, *J* = 8.5 Hz, 2H), 7.46-7.40 (m, 2H), 7.38-7.32 (m, 3H), 7.05 (d, *J* = 8.3 Hz, 1H), 6.97 (t, *J* = 7.5 Hz, 1H), 6.67 (t, *J* = 8.5 Hz, 2H), 3.43 (q, *J* = 7.1 Hz, 4H), 1.21 (t, *J* = 7.1 Hz, 6H).

Synthesis of the Cyclometallating ligand

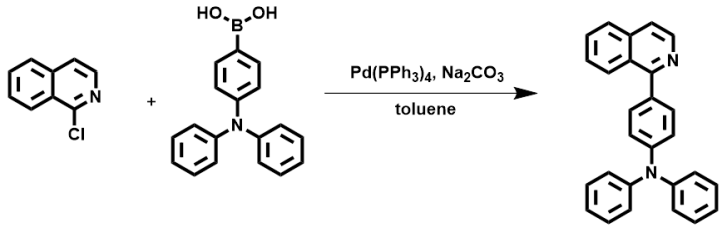

Scheme S3. Synthetic route for the cyclometallating ligand.

1-Chloroisoquinoline (0.496 g, 3.06 mmol) and 4-boronic acid triphenylamine (0.972 g, 3.36 mmol) were dissolved in toluene (30 mL) and tetrakis(triphenylphosphine)palladium(0) (0.177 g, 0.15 mmol) was added as a catalyst. Sodium carbonate (20 mL of 2 mol L^{-1} solution) was added and the mixture was refluxed for 48 h under N_2 protection. The mixture was then left to cool and extracted with dichloromethane. The organic phase was dried over anhydrous $MgSO_4$, and the crude product was purified by silica gel column chromatography (dichloromethane/petroleum ether, 10/3 v/v). A pure yellow solid was obtained in 74% yield. ^{1}H NMR (500 MHz, $CDCl_3$, δ [ppm]): 8.60 (d, J = 5.6 Hz, 1H), 8.24 (d, J = 8.5 Hz, 1H), 7.88 (d, J = 8.2 Hz, 1H), 7.70 (t, J = 8.1 Hz, 1H), 7.64-7.59 (m, 3H), 7.57 (t, J = 8.3 Hz, 1H), 7.32-7.27 (m, 4H), 7.25-7.8 (m, 6H), 7.07 (t, J = 8.1 Hz, 2H).

Synthesis of dichloro-bridged diiridium complex

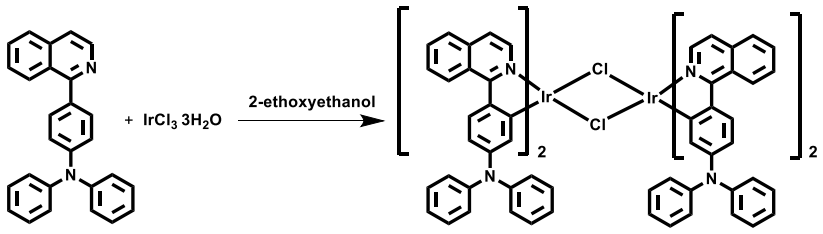

Scheme S4. Synthetic route for the dichloro-bridged diiridium complex.

The cyclometallating ligand (0.930 g, 2.5 mmol) and $IrCl_3$•$3H_2O$ (0.353 g, 1 mmol) were dissolved in a mixed solution of 2-ethoxyethanol (30 mL) and water (10 mL). The solution was heated to 120 °C and refluxed for 24 h under N_2. After the reaction was completed, it was cooled to room temperature; water was added to obtain a precipitate. The mixture was stirred for 5 min and filtered to obtain a solid. The solid was placed in an oven for 24 h to obtain a red solid with a yield of 80%. ^{1}H NMR

(500 MHz, $CDCl_3$, δ [ppm]): 8.87 (d, *J* = 6.4 Hz, 1H), 8.76 (d, *J* = 8.4 Hz, 1H), 7.89 (d, *J* = 8.8 Hz, 1H), 7.71-7.61 (m, 2H), 7.58 (d, *J* = 8.0 Hz, 1H), 6.84 (t, *J* = 8.4 Hz, 4H), 6.79-6.74 (m, 4H), 6.70-6.66 (m, 2H), 6.49 (dd, *J* = 8.8,2.5 Hz, 1H), 6.17 (d, *J* = 6.4 Hz, 1H), 5.53 (d, *J* = 2.4 Hz, 1H).

Synthesis of Ir-1-N

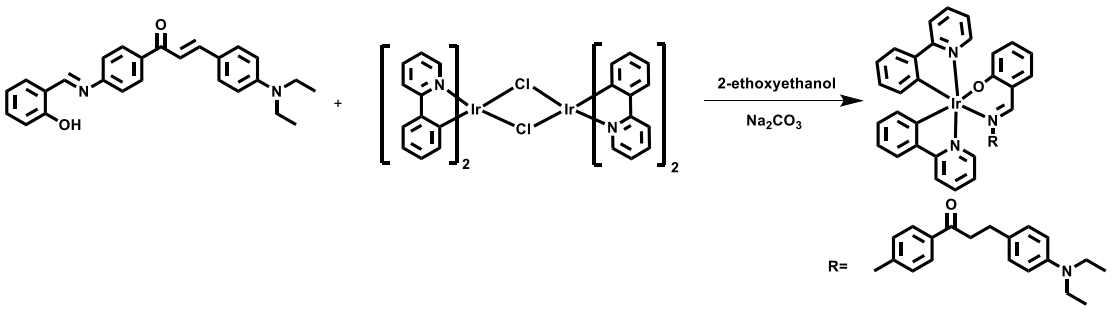

Scheme S5. Synthetic route for **Ir-1-N**. During the reaction the dichloro-bridged complex also acts as a catalyst to reduce the carbon-carbon double bond of the unsaturated ketone in **L2** to a carbon-carbon single bond.[2]

The dichloro-bridged diiridium complex (0.0536 g, 0.05 mmol), Schiff base ligand **L2** (0.0398 g, 0.1 mmol) and Na_2CO_3 (0.1745 g, 1.6 mmol) were added to 2-ethoxyethanol (25 mL). The mixture was heated to 140 °C under nitrogen atmosphere and refluxed for 8 h. After the reaction was completed, it was cooled to room temperature. Na_2CO_3 was removed by adding ethyl acetate. Using CH_2Cl_2 and petroleum ether as eluents (CH_2Cl_2/petroleum ether from 1/10 to 10/1, v/v), the crude product was purified by silica gel column chromatography. The complex **Ir-1-N** was obtained as an orange solid. Yield: 60%. ^{1}H NMR (500 MHz, $CDCl_3$, δ [ppm]): 8.88 (d, *J* = 6.7 Hz, 1H), 8.83 (d, *J* = 5.7 Hz, 1H), 8.08 (s, 1H), 7.88 (d, *J* = 8.1 Hz, 1H), 7.72 (t, *J* = 7.5 Hz, 1H), 7.69-7.64 (m, 1H), 7.58 (d, *J* = 7.7 Hz, 1H), 7.49 (d, *J* = 8.1 Hz, 1H), 7.33 (d, *J* = 3.7 Hz, 1H), 7.31 (d, *J* = 3.7 Hz, 1H), 7.25 (d, *J* = 2.0 Hz, 1H), 7.13 (dd, *J* = 8.0, 6.1 Hz, 2H), 7.09-7.02 (m, 3H), 6.69 (dd, *J* = 6.0, 3.1 Hz, 2H), 6.85

(t, *J* = 7.6 Hz, 1H), 6.74-6.67 (m, 3H), 6.65 (d, *J* = 8.6 Hz, 1H), 6.46-6.51 (m, 2H), 6.40 (t, *J* = 7.4 Hz, 1H), 6.25 (t, *J* = 7.6 Hz, 1H), 6.18 (t, *J* = 8.3 Hz, 2H), 6.16-6.14 (m, 1H), 3.34 (q, *J* = 7.1 Hz, 3H), 3.15 (q, *J* = 7.2 Hz, 1H), 3.03 (q, *J* = 7.1 Hz, 2H), 2.88-2.83 (m, 2H), 1.25 (t, *J* = 7.1 Hz, 2H), 1.15 (t, *J* = 7.0 Hz, 4H). ^{13}C NMR (151 MHz, $CDCl_3$) δ 197.89, 167.71, 167.36, 166.03, 160.07, 154.17, 148.82, 148.06, 147.29, 143.47, 143.03, 135.82, 135.76, 134.32, 133.57, 132.18, 132.15, 131.53, 128.35, 128.11, 128.04, 126.66, 123.90, 122.81, 122.49, 121.52, 120.67, 120.36, 120.34, 118.90, 117.98, 116.97, 112.70, 111.16, 43.39, 39.96, 28.42, 11.58. ESI-MS: [m/z] = 901.31 (M^+ + H) [calcd for $C_{48}H_{43}IrN_4O_2$ (M^+) 900.10]. The higher mass peak at 923 in Fig. S7 is from M^+ + Na.

Synthesis of Ir-2-N

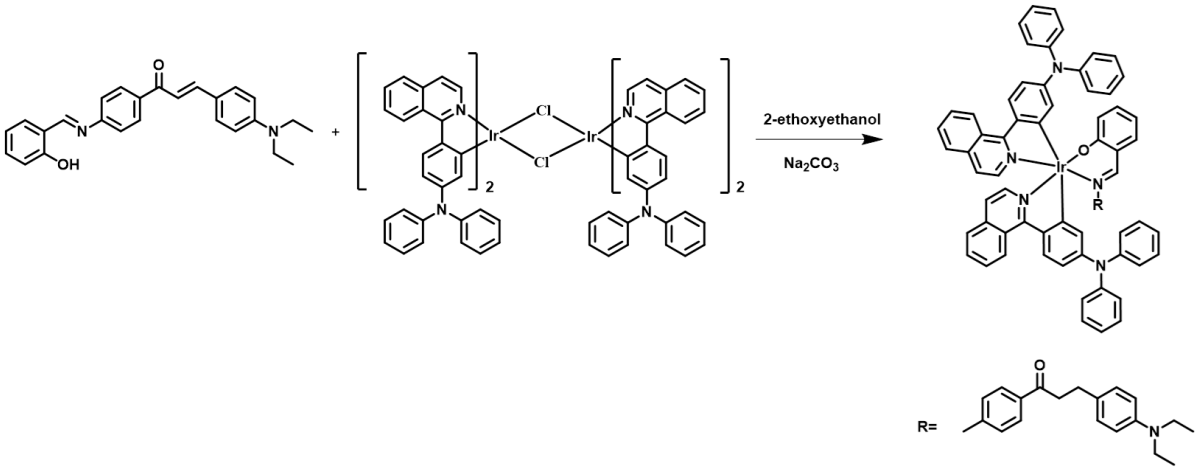

Scheme S6. Synthetic route for **Ir-2-N**. As in the synthesis of **Ir-1-N**, the dichloro-bridged complex also acts as a catalyst to reduce the carbon-carbon double bond in the unsaturated ketone of **L2** to a carbon-carbon single bond.[2]

The dichloro-bridged diiridium complex (0.0970 g, 0.05 mmol), Schiff base ligand **L2** (0.0398 g, 0.1 mmol) and Na_2CO_3 (0.1745 g, 1.6 mmol) were added to 2-ethoxyethanol (25 mL). The mixture was heated to 140 °C under nitrogen protection and refluxed for 8 h. After the reaction was completed, it was cooled to room temperature. Na_2CO_3 was removed by adding ethyl acetate. The obtained crude product was purified by column chromatography with ethyl acetate and petroleum

ether as eluents (ethyl acetate /petroleum ether from 1/10 to 10/1, v/v), and a red solid of complex **Ir-2-N** was obtained. Yield: 60%. ^{1}H NMR (500 MHz, $CDCl_3$, δ [ppm]): 8.72 (d, *J* = 8.4 Hz, 1H), 8.56 (d, *J* = 6.3 Hz, 1H), 8.45 (d, *J* = 6.4 Hz, 1H), 8.34 (d, *J* = 8.6 Hz, 1H), 8.04 (s, 1H), 7.95 (d, *J* = 8.9 Hz, 1H), 7.73 (d, *J* = 8.1 Hz, 1H), 7.69 (d, *J* = 7.9 Hz, 1H), 7.64-7.52 (m, 4H), 7.49 (d, *J* = 8.8 Hz, 1H), 7.39 (d, *J* = 8.2 Hz, 2H), 7.24-7.20 (m, 1H), 7.10 (t, *J* = 7.8 Hz, 3H), 7.03 (t, *J* = 8.0 Hz, 3H), 6.98-6.93 (m, 4H), 6.89 (dd, *J* = 8.5, 7.1 Hz, 4H), 6.85-6.81 (m, 4H), 6.79-6.75 (m, 4H), 6.75-6.71 (m, 3H), 6.66 (dd, *J* = 8.1, 6.7 Hz, 2H), 6.61 (d, *J* = 8.7 Hz, 2H), 6.58 (dd, *J* = 8.8, 2.5 Hz, 1H), 6.39-6.35 (m, 1H), 6.32 (dd, *J* = 8.8, 2.5 Hz, 1H), 6.22 (d, *J* = 8.0 Hz, 2H), 5.88 (d, *J* = 2.5 Hz, 1H), 5.66 (d, *J* = 2.4 Hz, 1H), 3.32 (q, *J* = 7.0 Hz, 4H), 3.08-3.01 (m, 2H), 2.88 (t, *J* = 7.8 Hz, 2H), 1.14 (t, *J* = 7.0 Hz, 6H). ^{13}C NMR (151 MHz, $CDCl_3$) δ 197.59, 167.45, 166.72, 165.83, 159.82, 154.83, 146.44, 145.75, 145.70, 140.18, 139.21, 137.91, 135.74, 135.59, 134.34, 133.43, 132.28, 129.33, 129.02, 128.73, 128.31, 128.15, 127.66, 127.54, 126.82, 126.61, 125.97, 125.21, 124.97, 124.61, 124.43, 124.29, 123.94, 123.73, 122.19, 121.98, 121.88, 120.37, 117.30, 117.25, 112.57, 112.37, 112.24, 111.19, 43.38, 40.01, 28.67, 28.39, 11.59. ESI-MS: [m/z] = 1335.4860 (M^+ +H) [calcd for $C_{80}H_{65}IrN_6O_2$ (M^+) 1334.63].

Preparation of Ir-1-N NPs and Ir-2-N NPs

Ir-1-N NPs and **Ir-2-N NPs** were prepared by the self-assembly of the Ir(III) complexes and poloxamer (F127). A solution of the corresponding Ir(III) complex (1 mg) and F127 (5 mg) in THF (3 mL) was added dropwise into deionized water (10 mL) under vigorous stirring within 30 min. Afterward, the mixture was stirred for a further 20 h to volatilize the residual THF thoroughly. Finally, the resulting mixture (**Ir-1-N NPs** or **Ir-2-N NPs**) was collected and stored at room temperature until use.

Preparation of $NaYF_4$@NaF:Yb,Tm@$NaYF_4$ UCNPs

Preparation of $NaYF_4$ Core UCNPs: According to the literature, bare-core UCNPs were prepared by the chloride solvothermal method.[3] The specific steps were as

follows: YCl_3•$6H_2O$ (1 mmol), oleic acid (6 mL) and octadecene (ODE) (15 mL) were added to a round-bottomed three-necked flask and then stirred at room temperature for 30 min in an argon atmosphere. The temperature was increased to 160 °C according to a certain temperature gradient with argon introduced, and stirred for 30 min, and then cooled to room temperature. NaOH (2.5 mmol), NH_4F (4 mol) and MeOH (4 mL) were added into another round-bottomed flask and ultrasound was used to promote dissolution. Then this mixed system was slowly added to the mixed solution in the previous step, heated to 75 °C, and stirred for 30 min to remove MeOH. The container was filled with argon to remove the air mixed in the previous step. The temperature of the mixed solution was raised to 300 °C according to a certain temperature gradient, and cooled to room temperature after the reaction for 90 min. The mixture was washed by centrifugation with acetone and methanol, respectively. After centrifugation, the product was dissolved in cyclohexane (8 mL).

Preparation of Yb, Tm shell materials: Yb and Tm (99.5% Yb, 0.5% Tm, 0.5 mmol), sodium trifluoroacetate (0.5mmol), oleic acid (3 mL) and ODE (7.5 mL) were mixed in the bottom three-neck flask and then stirred at 40 °C for 30 min with argon. The flask was heated to 120 °C, stirred for 30 min to remove water and the product was collected after cooling down.

Preparation of $NaYF_4$ shell materials: $Y(TFA)_3$, (1 mmol), sodium trifluoroacetate (0.5 mmol), oleic acid (3 mL) and ODE (7.5 mL) were added into a round-bottom three-necked flask and stirred at 40 °C for 30 min under argon. The flask was heated to 120 °C, stirred for 30 min to remove water and the product was collected after cooling down.

Preparation of $NaYF_4$@NaF:Yb, Tm@$NaYF_4$ UCNPs: $NaYF_4$ core (0.25 mmol), oleic acid (6 mL) and ODE (15 mL) were mixed in a round bottom flask and then heated to 85 °C and stirred for 30 min to remove cyclohexane from the mixture, then heated to 90 °C under argon for 30 min. The mixture was next heated up to 300 °C according to a certain temperature gradient. After stabilizing for 3-5 min, the spare shell raw materials were injected with a syringe, the Yb and Tm shell materials were injected in two batches (the first 5 mL, after the temperature reached 300 °C and

continue for 15 min, then 5.5 mL was injected for the second time), and the temperature was returned to 300 °C and the reaction was continued for 45 min. Then, the $NaYF_4$ shell material was injected in four batches. Finally, the system was cooled to room temperature, and the product was washed and collected by the same process as in the preparation of $NaYF_4$ core UCNPs, to obtain $NaYF_4$@NaF:Yb, Tm@$NaYF_4$ UCNPs.

Preparation of UCNPs@Ir-2-N

UCNPs@Ir-2-N was prepared by a filming-rehydration method. UCNPs (0.5 mL) were added to EtOH (0.5 mL), and the mixture was then centrifuged at 6500 rpm for 6 min to remove the supernatant. The precipitate, **Ir-2-N** (1 mg) and TPGS (50 mg) were dissolved in chloroform (1 mL). After the solvent was evaporated under reduced pressure, deionized water (1 mL) was added, and the system was heated in a water bath for10 min to fully hydrate followed by centrifugation at 12000 rpm for 20 min. By filtration through a 0.22 μm filter, uniformly dispersed **UCNPs@Ir-2-N** was obtained. According to the original feed ratio of **UCNPs@Ir-2-N** and the standard curve of **Ir-2-N** (Fig. S16), the relationship between the concentration of **UCNPs@Ir-2-N** and **Ir-2-N** was approximately estimated:[4] (1 μg mL^{-1} **Ir-2-N** was in 70 μg mL^{-1}) **UCNPs@Ir-2-N**. The concentration of **Ir-2-N** was used to quantify the concentration of **UCNPs@Ir-2-N** in the ensuing experiment in this communication.

Test Methods for Singlet Oxygen Generation in Solution

The effect of PDT can be evaluated by the $^1O_2$ generation capacity in the solution. In these experiments, ICG was used as an indicator to evaluate the $^1O_2$ generation capacity of **Ir-1-N** and **Ir-2-N** and the corresponding NPs in solution.[5] **Ir-1-N** and **Ir-2-N** and their corresponding NPs solutions (15 μg mL^{-1}) were mixed with ICG solution (5 μg mL^{-1}) as working solutions. The working solution (3 mL) was transferred to a cuvette, and then was illuminated with a 425 nm LED at 20 mW cm^{-2} for 300 s. **UCNPs@Ir-2-N** (15 μg mL^{-1}) was mixed with the ICG solution (5 μg mL^{-1})

and the mixture was transferred to a cuvette, and then was illuminated with 980 nm laser at 0.6 W cm^{-2} for 30 min.

Cell culture methods

Mouse breast cancer cells (4T1 cells) were selected as the cell model for these experiments. The culture medium was prepared by RPMI Medium 1640 containing 10% (v:v) FBS. The cell culture flask was placed in an incubator at 37 °C and 5% CO_2. To ensure adequate nutrition for the cells, the culture medium was changed every two days.

Cytotoxicity test methods

The cytotoxicity of **UCNPs@Ir-2-N** was detected by MTT.[6] 4T1 cells were seeded in 96-well plates at a density of 10,000 cells per well. The cells were cultured in the incubator at 37 °C and 5% CO_2 for 24 h. After aspirating the old culture medium, RPMI Medium 1640 (100 μL) containing different concentration gradient PSs (0-15 μg mL^{-1}) were added to each well. The original culture medium was replaced by fresh RPMI Medium 1640 (100 μL) after 6 h. The light group was irradiated 5 times with a 980 nm laser at 0.6 W cm^{-2} for 2 min each time, while the dark group was not illuminated. The time between irradiation periods was 10 min to avoid overheating the cells at 980 nm. After irradiation, the cells were placed in the incubator for 24 h. MTT (10 μL) with the concentration of 5 mg mL^{-1} was added to each well. The cells were placed in the incubator for 4 h. After 4 h, DMSO (200 μL) was added to each well to replace the original medium. The absorbance value of the sample at 490 nm was detected by a microplate reader.

Live/Dead Staining Test Methods[7]

4T1 cells were seeded in confocal dishes at the density of 50,000 cells per well and incubated for 24 h. After the culture medium was aspirated, RPMI Medium 1640 containing **UCNPs@Ir-2-N** (15 μg mL^{-1}) was added to the confocal dish. After

culturing for 2 min 5 times the culture medium containing **UCNPs@Ir-2-N** was removed and fresh RPMI Medium 1640 was added. The light group was irradiated with 980 nm laser at 0.6 W cm^{-2} for 2 min 5 times, and the dark group was treated the same without illumination. After illumination, the confocal dish was placed in the incubator and continued to be incubated overnight. PBS was used to wash the confocal dishes. Detection buffer containing Calcein-AM and PI was added to the confocal dishes. This was followed by incubation in the dark in the incubator for 30 min. The fluorescence image was observed under an inverted fluorescence microscope to judge the cell survival state.

Test methods for endocytic behavior

4T1 cells were seeded in confocal culture dishes at a density of 50,000 cells per well. A cell suspension (1 mL) containing RPMI Medium 1640 was added to each well. The cells were then placed in an incubator at 37 °C and 5% CO_2 overnight. The original medium was replaced by RPMI Medium 1640 containing **UCNPs@Ir-2-N** (15 μg mL^{-1}). The incubation time was 0.5 h, 2 h and 6 h, respectively. After incubation, the supernatant was withdrawn and the confocal culture dish was washed twice with PBS, and the uptake of **UCNPs@Ir-2-N** by cells was observed by CLSM under 980 nm.

Evaluation of intracellular singlet oxygen production capacity

The ability of PSs to generate intracellular $^1O_2$ was assessed by DCFH-DA.[8] 4T1 cells were seeded in confocal dishes at a density of 50,000 cells per well and incubated for 24 h. The next procedure was to aspirate the original medium and add RPMI Medium 1640 (1 mL) containing **UCNPs@Ir-2-N** (15 μg mL^{-1}) to the confocal dish. After continuing to culture in the incubator for 6 h, the supernatant was removed and RPMI 1640 was added. The light group was irradiated 5 times with a 980 nm laser at 0.6 W cm^{-2} for 2 min each time, and the dark group was treated in the same way without illumination. After light exposure, the original medium was aspirated, washed twice

with PBS, and then DCFH-DA (1 μL) was dissolved in blank RPMI Medium 1640 without FBS and added to the confocal culture dish. After treatment in the dark for 20 min, the medium containing DCFH-DA was aspirated, washed twice with PBS (1 mL). And then, PBS (1 mL) was added, followed by CLSM to observe the green fluorescence intensity in the cells.

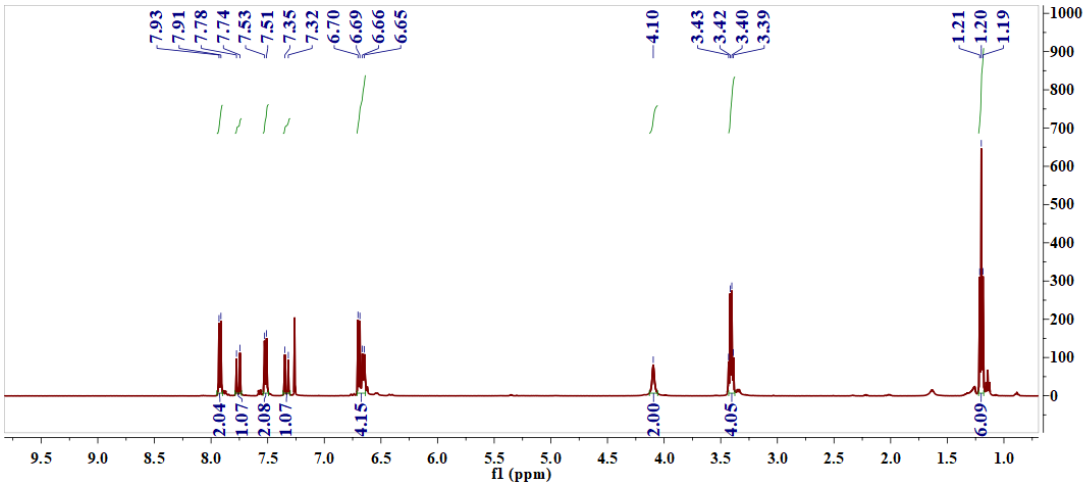

Fig. S1. ^{1}H NMR spectrum of **L1** in $CDCl_3$ at room temperature.

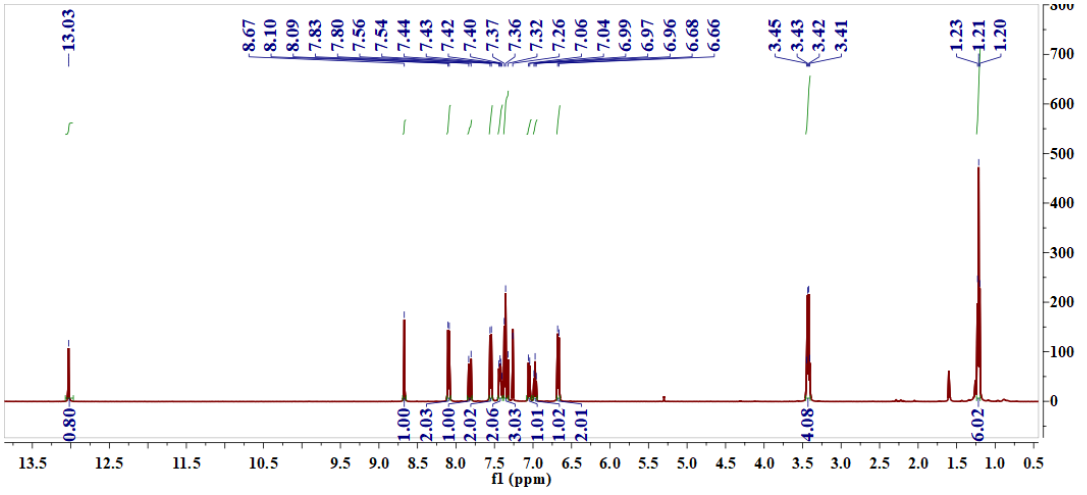

Fig. S2. ^{1}H NMR spectrum of **L2** in $CDCl_3$ at room temperature.

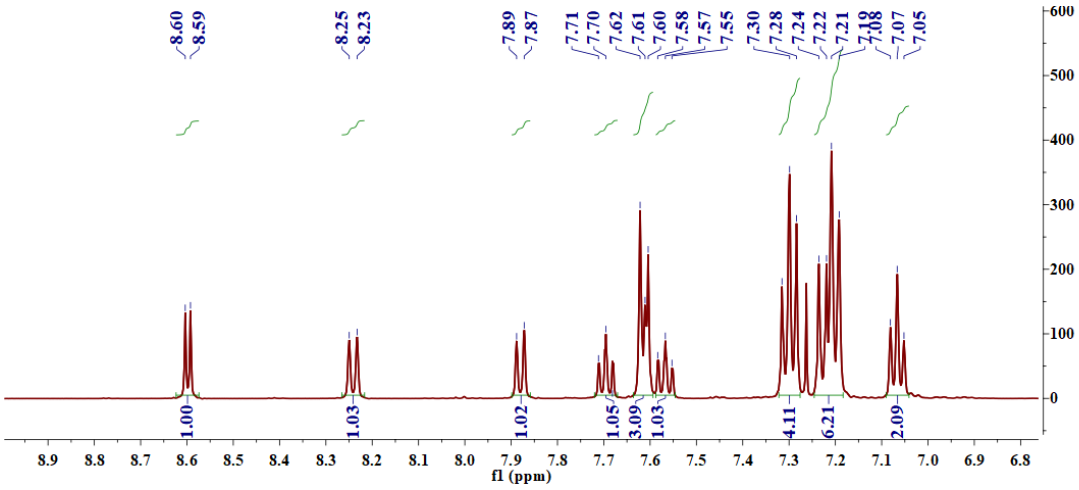

Fig. S3. ^{1}H NMR spectrum of the cyclometallating ligand in $CDCl_3$ at room temperature.

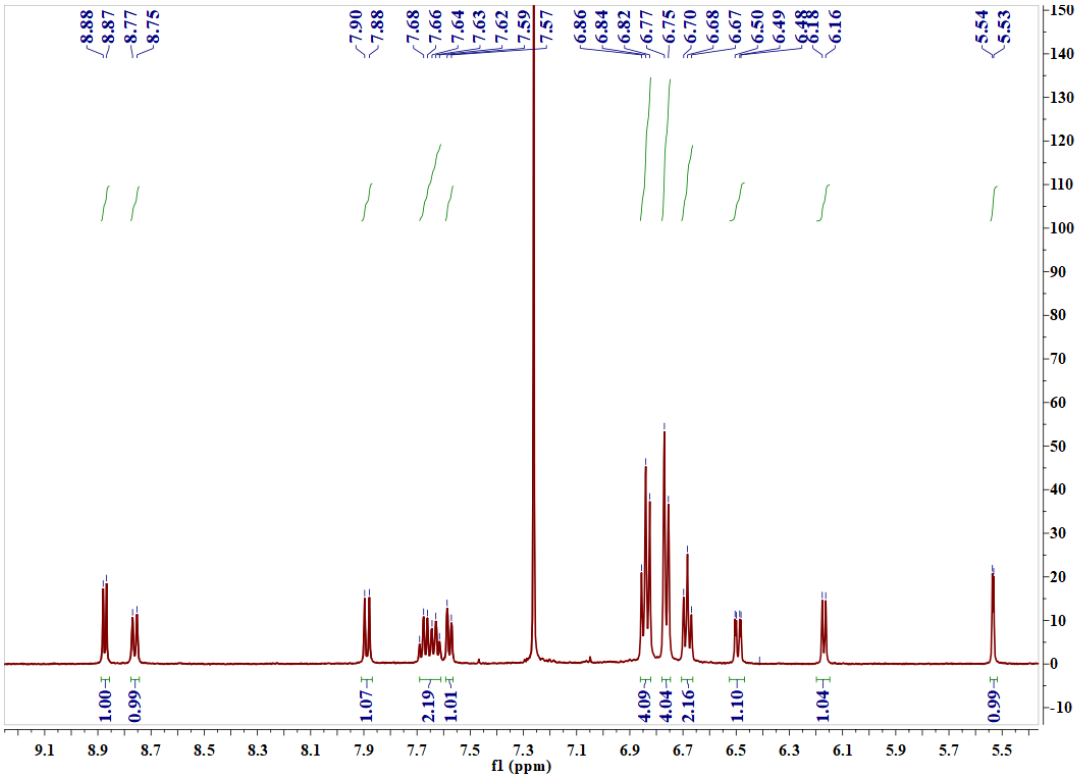

Fig. S4. ^{1}H NMR spectrum of the dichloro-bridged diiridium complex in $CDCl_3$ at room temperature.

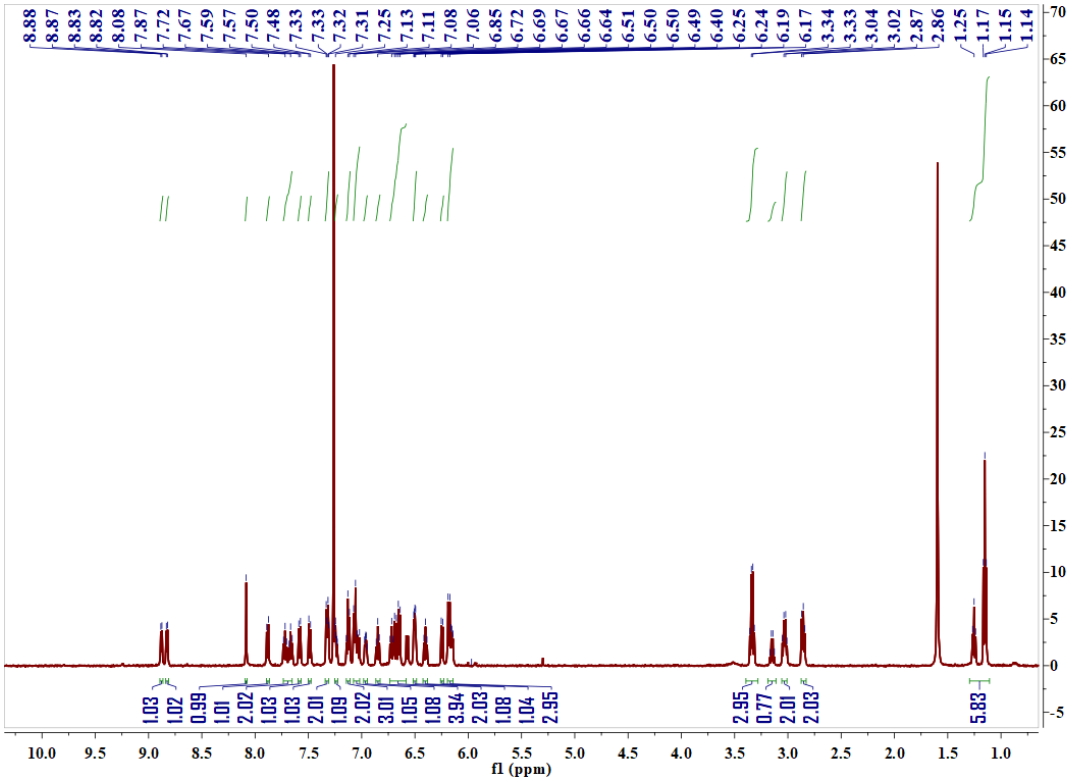

Fig. S5. ^{1}H NMR spectrum of **Ir-1-N** in $CDCl_3$ at room temperature.

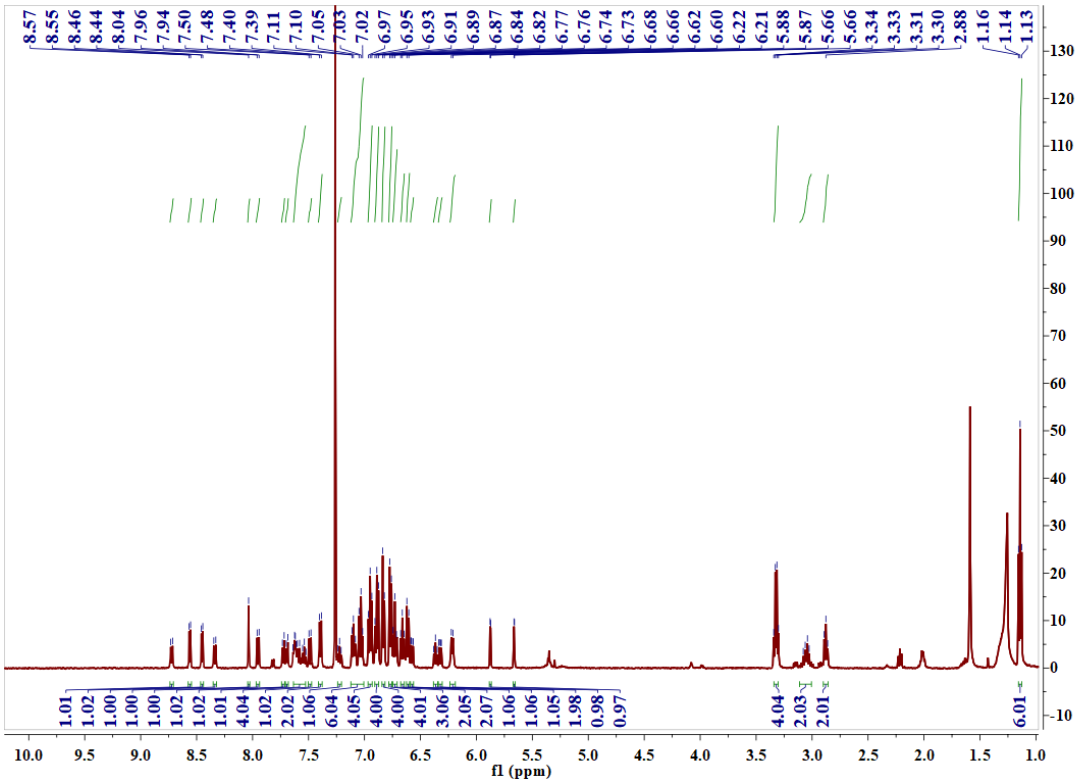

Fig. S6. ^{1}H NMR spectrum of **Ir-2-N** in $CDCl_3$ at room temperature.

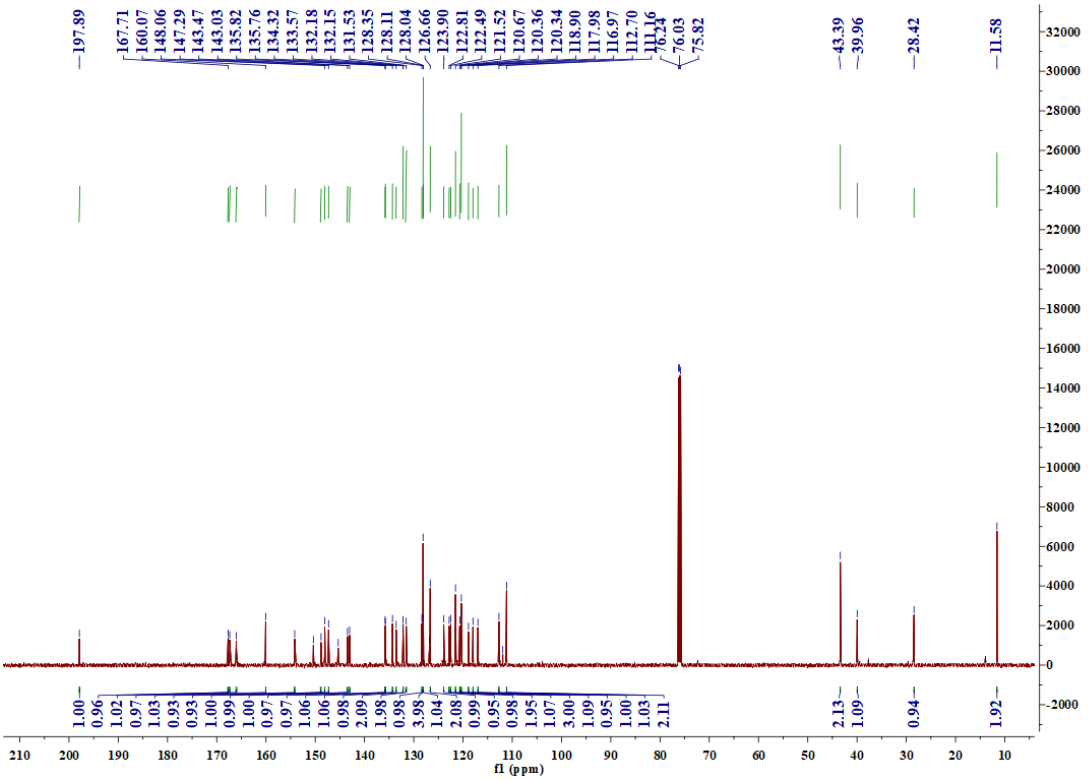

Fig. S7. ^{13}C NMR spectrum of **Ir-1-N** in $CDCl_3$ at room temperature.

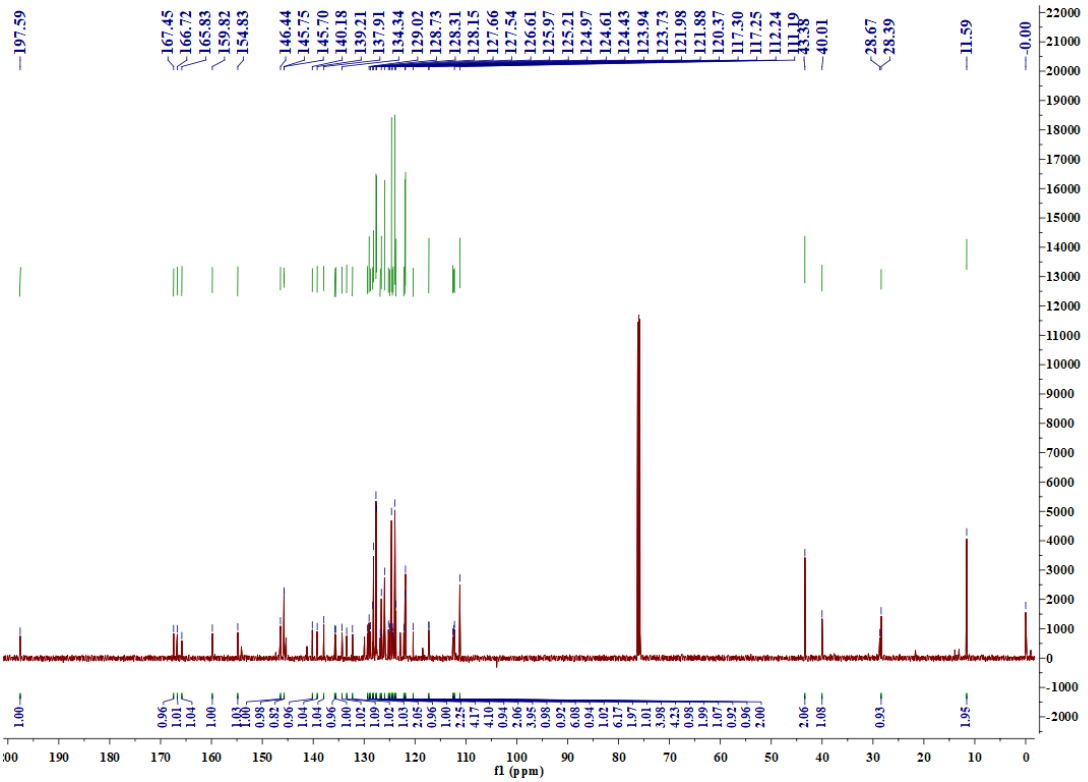

Fig. S8. ^{13}C NMR spectrum of **Ir-2-N** in $CDCl_3$ at room temperature.

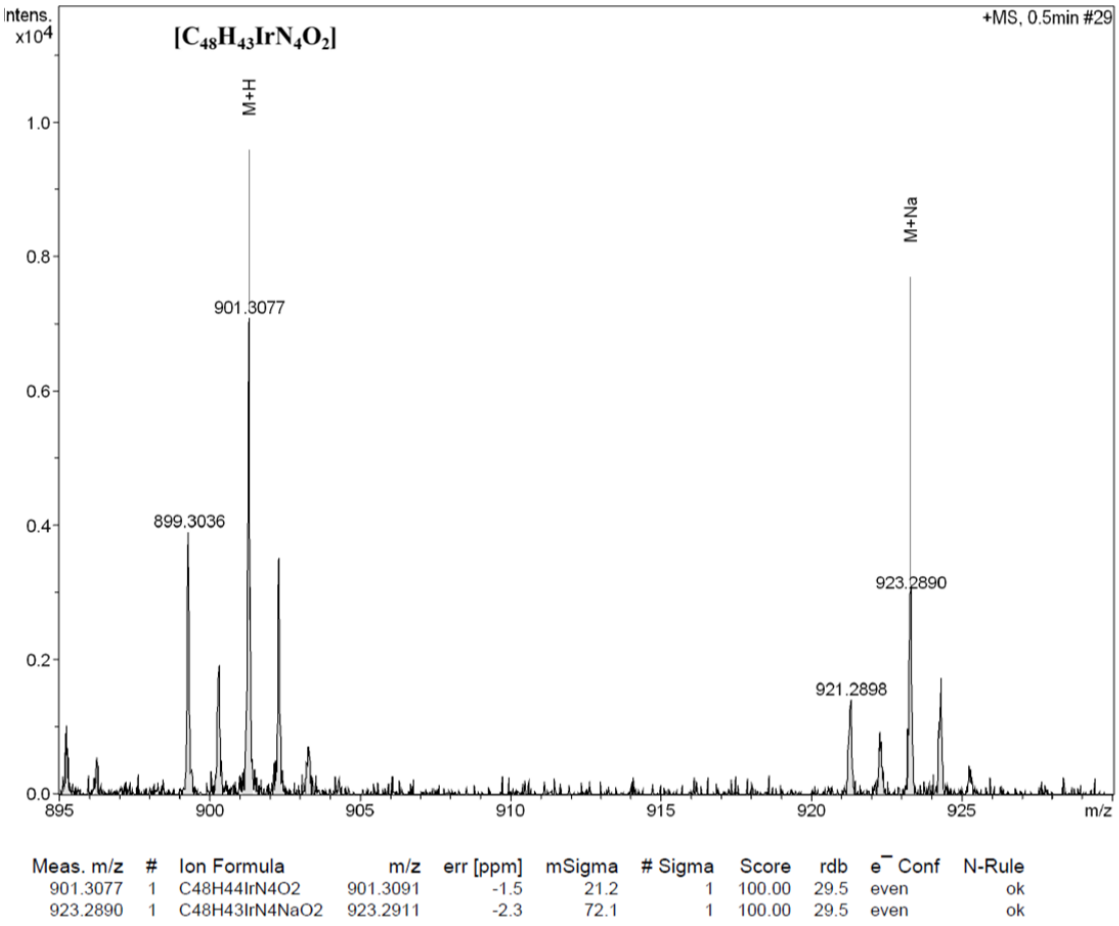

Meas. m/z	#	Ion Formula	m/z	err [ppm]	mSigma	# Sigma	Score	rdb	e⁻ Conf	N-Rule
901.3077	1	C48H44IrN4O2	901.3091	-1.5	21.2	1	100.00	29.5	even	ok
923.2890	1	C48H43IrN4NaO2	923.2911	-2.3	72.1	1	100.00	29.5	even	ok

Fig. S9. High Resolution Mass Spectrometry (HRMS) of **Ir-1-N**.

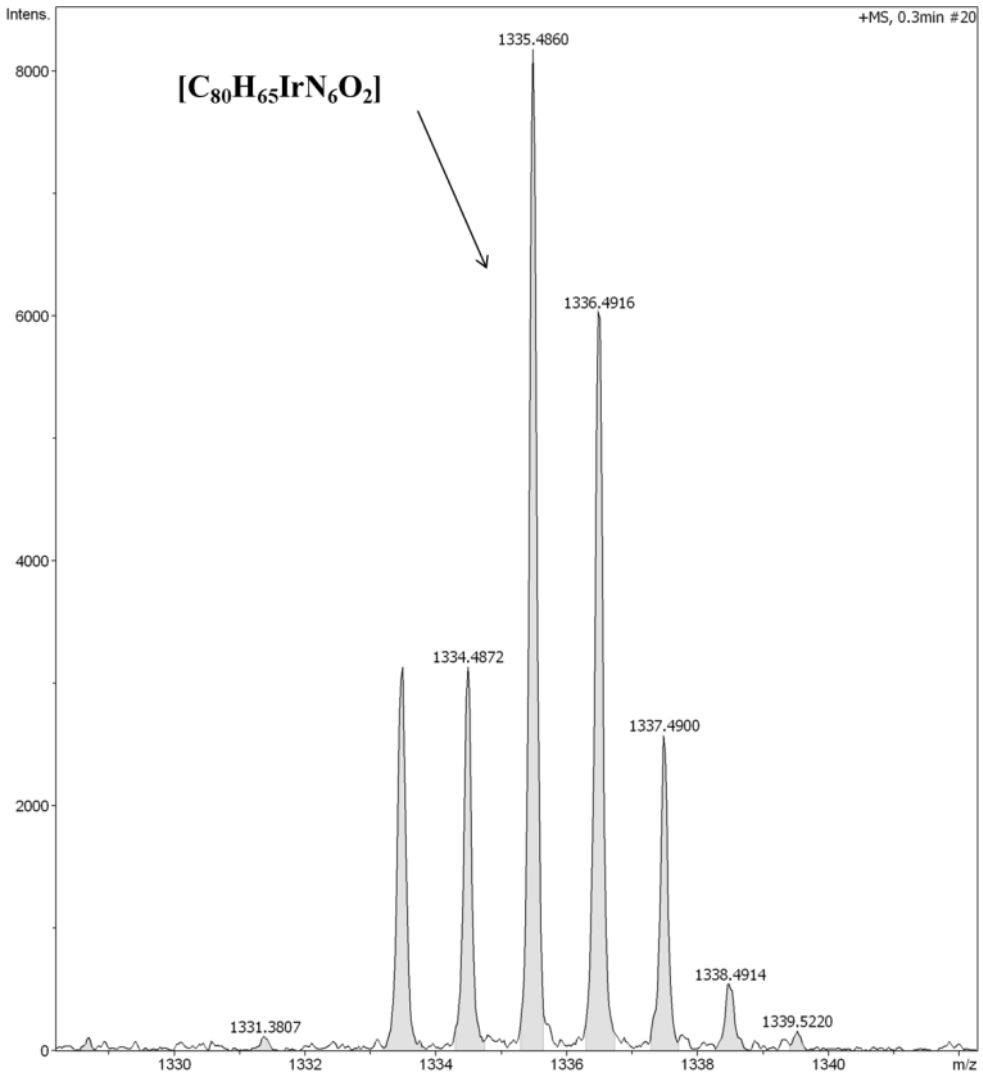

Fig. S10. High Resolution Mass Spectrometry (HRMS) of **Ir-2-N**.

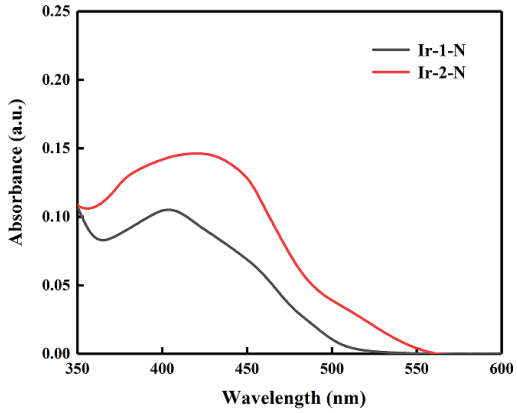

Fig. S11. The expanded UV–vis absorption spectra (350-600 nm) of **Ir-1-N** and **Ir-2-N** (10^{-5} M) in CH_3CN.

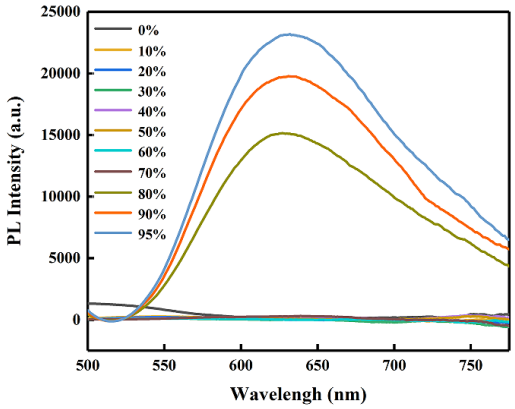

Fig. S12. PL spectra of **Ir-1-N** in CH_3CN–H_2O mixtures (complex concentration = 1.0×10^{-5} M) with different water fractions (0–95% v/v) at room temperature.

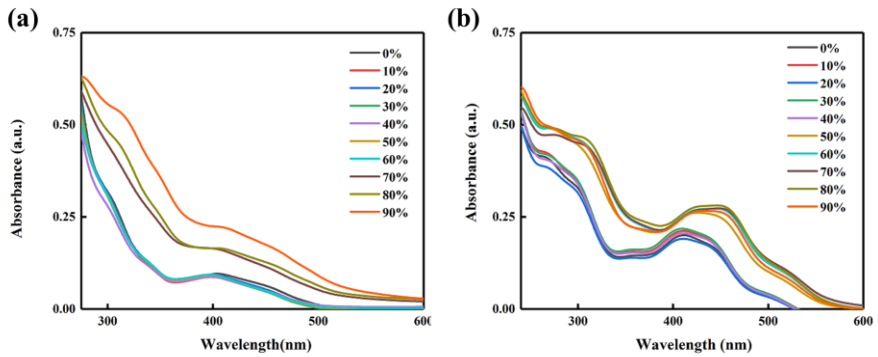

Fig. S13. The UV–vis absorption spectra of **Ir-1-N** and **Ir-2-N** CH_3CN-H_2O mixtures (complex concentration = 1.0×10^{-5} M) with different water fractions (0–90% v/v) at room temperature.

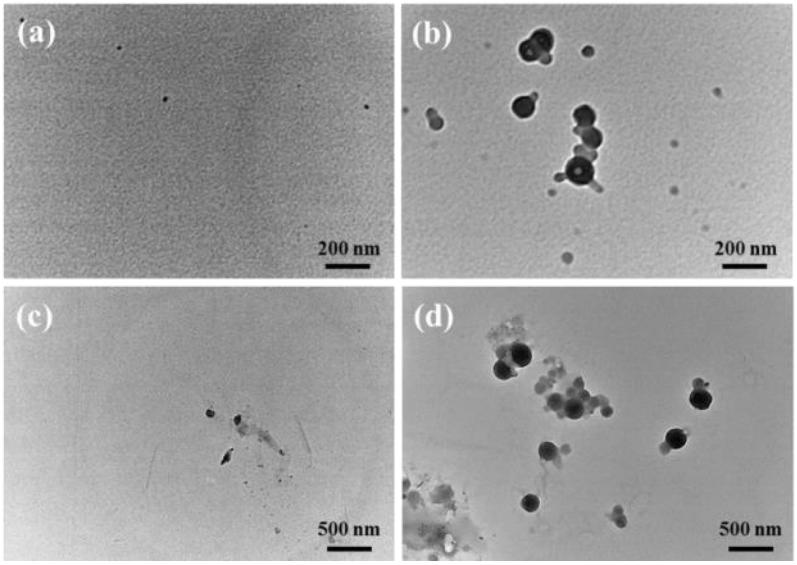

Fig. S14. The TEM images of **Ir-1-N** in CH_3CN (a) and in CH_3CN-H_2O mixture (99% H_2O) (b). The TEM images of **Ir-2-N** in CH_3CN (c) and in CH_3CN-H_2O mixture (99% H_2O) (d).

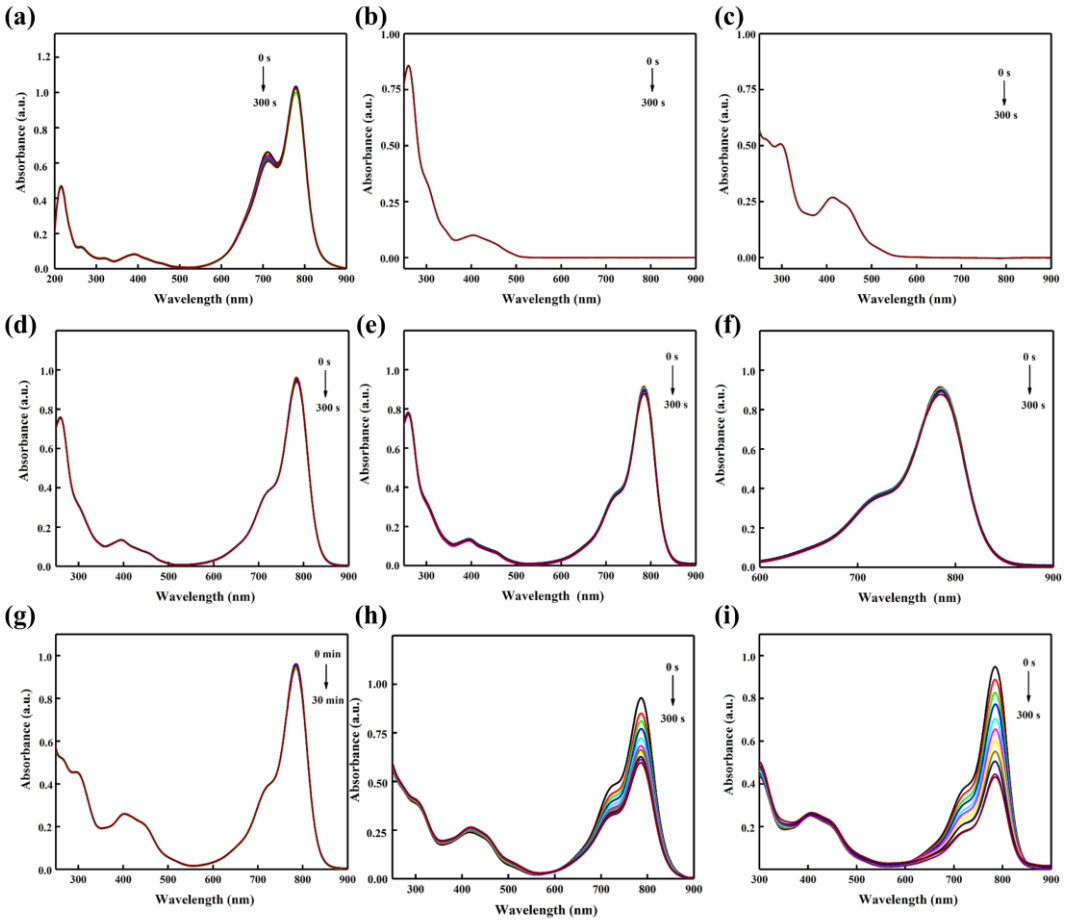

Fig. S15. UV–vis absorption spectra of ICG (5 μg mL^{-1}) (a) upon exposure to light illumination (425 nm, 20 mW cm^{-2}); UV–vis absorption spectra of **Ir-1-N** (b) and **Ir-2-N** (c) upon exposure to light illumination (425 nm, 20 mW cm^{-2}). UV–vis absorption spectra of ICG (5 μg mL^{-1}) (d) in the presence of **Ir-1-N** under dark conditions; (e) in the presence of **Ir-1-N** upon illumination (425 nm, 20 mW cm^{-2}); f) The expanded spectra (600-900 nm) of (e). UV–vis absorption spectra of ICG (5 μg mL^{-1}) (g) in the presence of **Ir-2-N** under dark conditions; (h) in the presence of **Ir-2-N** upon illumination (425 nm, 20 mW cm^{-2}). (i) The expanded spectra (600-900 nm) of (h). The control groups are (a), (d) and (g).

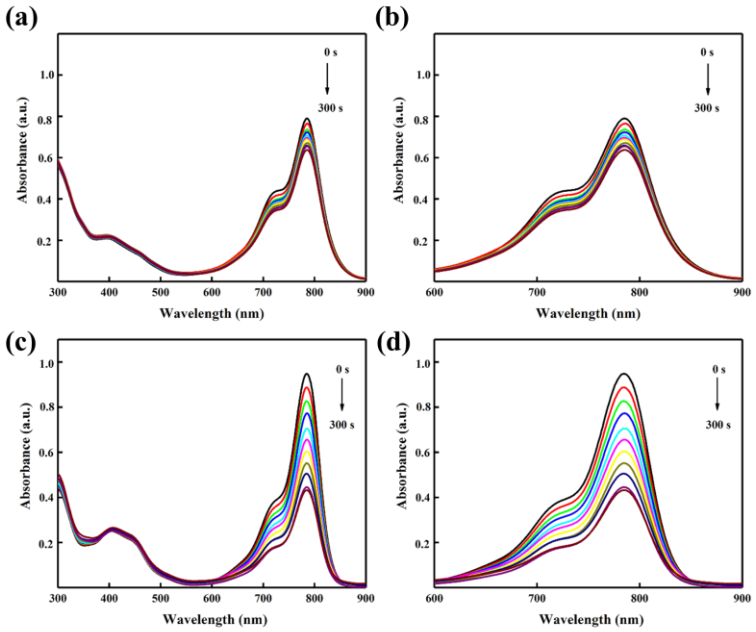

Fig. S16. (a) UV–vis absorption spectra of ICG (5 μg mL^{-1}) upon illumination (425 nm, 20 mW cm^{-2}) in the presence of **Ir-1-N NPs** (a) and **Ir-2-N NPs** (c). (b) The expanded spectra (600-900 nm) of (a). (d) The expanded spectra (600-900 nm) of (c).

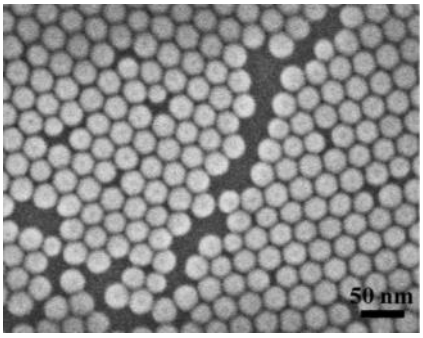

Fig. S17. SEM image of UCNPs.

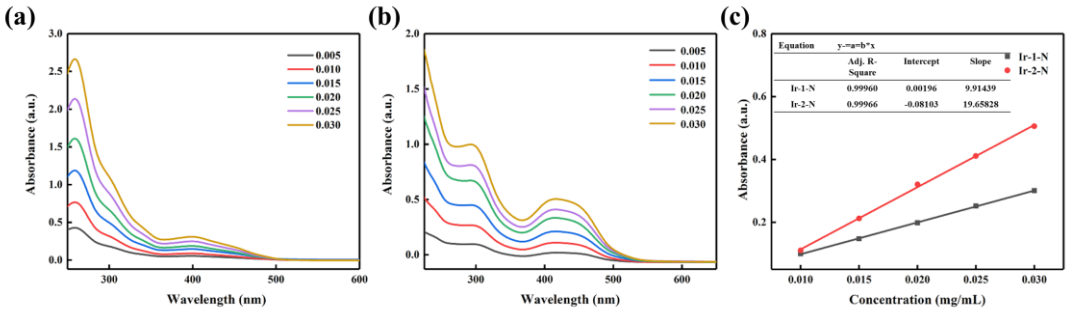

Fig. S18. UV–vis absorption spectra of **Ir-1-N** (a) and **Ir-2-N** (b) in different concentration (mg/mL) in CH_3CN/H_2O = 4/1 (v/v). (c) Standard curve of **Ir-1-N** and **Ir-2-N** in CH_3CN/H_2O = 4/1 (v/v).

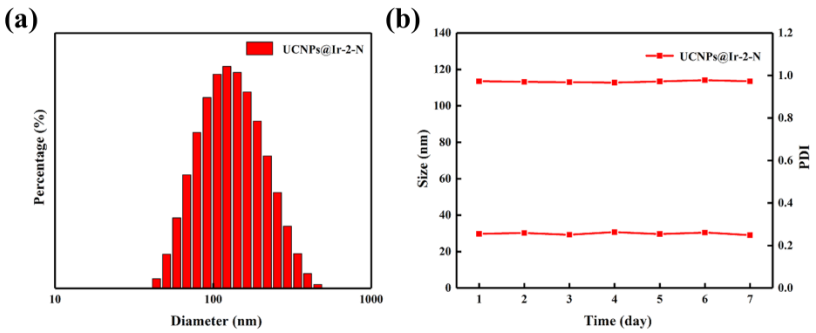

Fig. S19. (a) DLS data for **UCNPs@Ir-2-N**. (b) DLS data for **UCNPs@Ir-2-N** during 7 days.

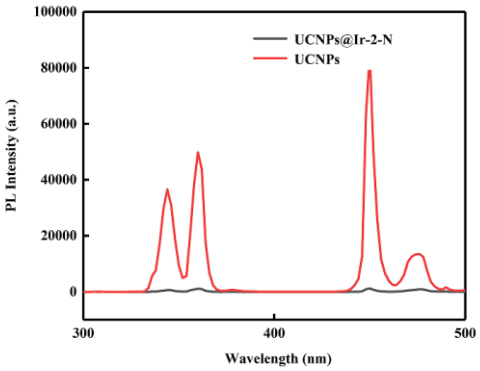

Fig. S20. (a) The enlarged PL spectra (300-500 nm) of UCNPs and **UCNPs@Ir-2-N**.

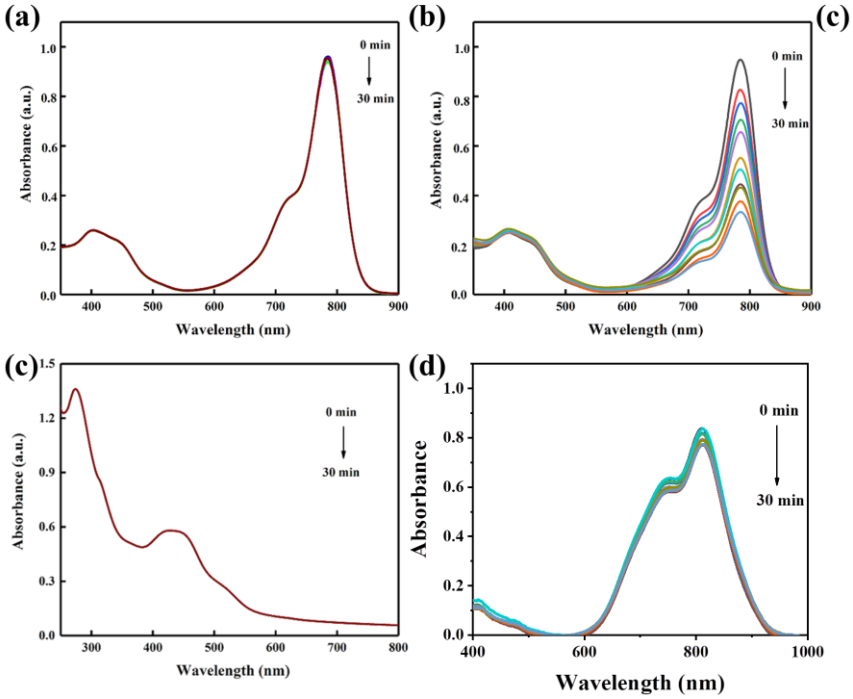

Fig. S21. UV–vis absorption spectra of ICG (5 μg mL^{-1}) (a) in the presence of **UCNPs@Ir-2-N** under dark conditions; (b) in the presence of **UCNPs@Ir-2-N** upon laser irradiation (980 nm, 0.6 W cm^{-2}); (c) UV–vis absorption spectra of **UCNPs@Ir-2-N** upon laser irradiation (980 nm, 0.6 W cm^{-2}); (d) UV–vis absorption spectra of ICG (5 μg mL^{-1}) in the presence of UCNPs upon laser irradiation (980 nm, 0.6 W cm^{-2}).

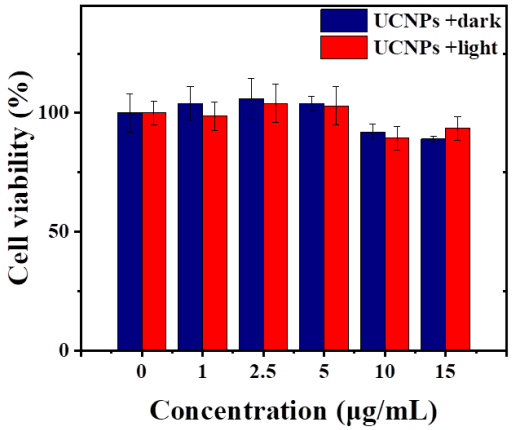

Fig. S22. Relative viability of 4T1 cells after 24 h co-incubation with UCNPs under darkness and under irradiation (980 nm, 0.6 mW cm^{-2}).

Table S1 Photophysical data of **Ir-1-N** and **Ir-2-N**

	λ_{abs} (nm)	λ_{em} (nm)	Φ_p (%)	τ_P (μs)	ε (m^{-1} cm^{-1})
Ir-1-N[a]	255; 400	640	16.6	0.56	10552
Ir-2-N[a]	300; 415	660	18.9	0.62	15574

[a]Measured in MeCN/water (v/v = 1/9), concentration: 1.0×10^{-5} M, λ_{ex} = 425 nm

References

1. Y. Liu, N. Song, L. Chen, S. Liu and Z. Xie, *Chem. Asian J.*, 2018, **13**, 989-995.
2. K. Zhang, L. Q. Lu, Y. Jia, Y. Wang, F. D. Lu, F. Pan and W. J. Xiao, *Angew. Chem. Int. Ed.*, 2019, **58**, 13375-13379.
3. H.-S. Qian and Y. Zhang, *Langmuir*, 2008, **24**, 12123-12125.
4. S. Z. Ren, B. Wang, X. H. Zhu, D. Zhu, M. Liu, S. K. Li, Y. S. Yang, Z. C. Wang and H. L. Zhu, *ACS Appl. Mater. Interfaces*, 2020, **12**, 24662-24674.
5. L. Zhang, Y. Li, W. Che, D. Zhu, G. Li, Z. Xie, N. Song, S. Liu, B. Z. Tang, X. Liu, Z. Su and M. R. Bryce, *Adv. Sci.*, 2019, **6**, 1802050.
6. D. Kessel and J. J. Reiners, *Autophagy*, 2020, **16**, 2098-2101.
7. M. Li, T. Xiong, J. Du, R. Tian, M. Xiao, L. Guo, S. Long, J. Fan, W. Sun, K. Shao, X. Song, J. W. Foley and X. Peng, *J. Am. Chem. Soc.*, 2019, **141**, 2695-2702.
8. F. Wu, M. Yang, J. Zhang, S. Zhu, M. Shi and K. Wang, *J. Biol. Inorg. Chem.*, 2019, **24**, 53-60.